Indian J. Phys. **67A** (3), 237-250 (1993)

Small angle X-ray scattering investigation of tasar using correlation functions

T Misra, T Patel, A K Sahoo*, Md N Khan and V H Buch**
Regional Engineering College, Rourkela-769008, Orissa, India

Received 28 May 1992, accepted 6 January 1993

Abstract : Due to the immense importance of Indian tasar (Antheraea mylitta) as a textile fibre, attempts have been made in this work to highlight various macromolecular parameter of air dried tasar (T_a) and heat treated tasar (T_{60}) using small angle X-ray scattering (SAXS), treating the samples as densely packed micellar structures by using the theory of Vonk. The analysis of SAXS intensities of T_a and T_{60} samples shows marked deviation from Porod's law indicating that the fibre is not an ideal two-phase system but rather is a non-ideal two-phase structure characterized by continuous electron density variation at the phase boundaries over a distance 'E' known as the width of the transition layer. The width/thinkness 'E' of the transition region was found by employing Vonk and Ruland methods. The use of correlation functions introduced by Debye and Bueche is considered as the most general approach for the analysis of SAXS data. Hence one- and three-dimensional correlation functions have been used to obtain parameters like D, the average probable distance between dense particles transverse to the layers; S/V the specific inner surface; ϕ_1 and ϕ_2, the volume fractions of matter and void respectively; $\bar{l}_1$ and $\bar{l}_2$, the transversal lengths; $\bar{l}_r$, the range of inhomogeneity; l_c the length of coherence; f_c, the characteristic number and $2E/D$, the volume fraction of transition layer.

Keywords : Non-ideal two-phase system, thickness of transition layer, correlation function, tasar fibre, small angle X-ray scattering.

PACS Nos. : 78.70.Ck, 42.81.Cn

1. Introduction

The small angle X-ray scattering (SAXS) technique is being extensively used in studying natural fibres such as silk, sisal, jute and synthetic fibres like nylon, rayon and various other polymers. According to Porod's law [1], the scattered X-ray intensity at the tail end of the SAXS curve decreases in proportions to s^{-4} for ideal two-phase structures having sharply defined phase boundaries, where 's' is the radial coordinate in reciprocal space. Investigations [2,3] of SAXS intensity pattern from natural and artificial fibres show a remarkable deviation from the Porod's law i.e. the intensity in the tail end of the SAXS curve is observed to decrease in proportion to s^{-6} rather than s^{-4}. This deviation has been explained by many workers and ultimately Ruland [4] put forward a novel method for

Rourkela Institute of Technology, Kalunga-770 031, Orissa, India.
* Department of Chemical Technology, Bombay University, Matunga, India.

explaining the deviation from Porod's law in terms of a non-ideal two-phase model which is taken as a system characterized by continuous electron density variation on the phase boundaries between matter and void phases in the interior of the scatterer.

In the non-ideal two-phase system the region over which the electron density variation takes place is known as width of transition layer E. As tasar is a macromolecular system, being proteinous in nature, a small angle X-ray study has been undertaken to determine some of the macromolecular parameters associated with these fibres following the procedure of Heyn [5,6].

2. Sample and its importance

Tasar silk was obtained from the cocoon of tasar by the improved tasar cooking technique [7]. The sample under investigation was collected from the Central Silk Research and Training Centre, Bangriposi, Mayurbhanj, Orissa, India. The sample was dewaxed by using the process reported by Ratho *et al* [8] and the dewaxed tasar silk fibre has an amino acid composition of various fibroins of about 100%, after all other constituents being separated out.

3. Experimental

The SAXS data were collected by means of a compact Kratky camera 'Anton Paar K G A -8054 GRAZ AUSTRIA-EUROPA' using a 'Phillips' PW 1729 X-ray Generator having a copper target operated at 40 KV ad 30 mA. The entrance slit and counter slit width of the camera were adjusted at 150 μm and 375 μm respectively. The X-ray after passing through nickel filter was used for irradiating the samples. The intensity data for the air dried sample of tasar (hence forward named as T_a) and heat treated sample of tasar 60°C (hence forward named as T_{60}) were collected as described below. The samples were inserted into two Mark Capillary tubes of diameter 0.7 mm each for collecting the intensity data. The capillary tube was aligned so as to make its length parallel to the length of the primary beam thereby making the fibres parallel to primary beam. A SAXS pattern of the sample was also recorded mounting it perpendicular to the beam. Filtered X-ray Cuk$_\alpha$ ($\lambda = 1.54$ Å) is usually used as used in powder method in X-ray crystallography [9,10] considering it to be almost monochromatised. Radiation was allowed to fall on the samples. The body of the compact camera contains a tightly sealed evacuated space which encases all the construction devices, except the scattered intensity recording counter device. A proportional counter was used to record the scattered intensity. The incident X-rays enter the evacuated space through a 0.25 mm thick Beryllium Window from the front side and the scattered X-rays emerge out through a similar window at the opposite end. Due to this design, the radiation path between the two windows runs through a vacuum of about 0.5 torr, thus avoiding parasitic scattering by air molecules. The scattered radiation crosses the Beryllium Window through different lengths at different positions depending on the scattering angle, so that variation in the absorption by the window would cause errors in the absolute scattering intensities. But practically errors due to this effect are below 0.5% and hence can be regarded as negligible.

The distance from the sample to the counter slit was 20 cm and the temperature was maintained at 22.5°C by the help of an air conditioner during X-ray intensity data collection for the samples T_a and T_{60}.

4. Theory

For a non-ideal two-phase system having continuous electron density variation at the phase boundary. Vonk [11] established the relation between the amplitude 'F' expressed in absolute units of scattered X-ray at non-zero angle to the deviation η of the electron density from the mean value as

$$\eta(r) = \int F(s) \exp(2\pi i r s) dv_s = T_f F(s) \tag{1}$$

where r is a vector in real space with coordinates x, y, z; s is a vector in reciprocal or Fourier space with coordinates u, v, w; dv_s is a volume element given by $dudvdw$ and T_f is an operator indicating Fourier transformation. The domain of integration in reciprocal space is carried out over the samll angle X-ray scattering intensities whereas in real space, it is carried out for the irradiated volume of the sample. Differentiation of $\eta(r)$ with x, y, z and application of Parseval's theorem [2,3] leads to the following relations.

$$16\pi^3 \int_0^\infty s^4 I(s) ds = \int_0^\infty |\text{grad}\eta^2| \, dv_r \tag{2}$$

$$4\pi \int_0^\infty s^2 I(s) ds = \int_0^\infty \eta^2 dv_r \tag{3}$$

where $\int_0^\infty s^2 I(s) ds$ is usually called the desmeared invariant. The intensities obtained are not in absolute units, hence the ratio of the relations (2) and (3) gives a very useful parameter

$$R = \frac{\langle|\text{grad}\eta|^2\rangle}{\langle\eta^2\rangle} = 4\pi^2 \frac{\int_0^\infty s^4 I(s) ds}{\int_0^\infty s^2 I(s) ds}$$

$$= 6\pi \frac{\int_0^\infty s^3 \bar{I}(s) ds}{\int_0^\infty s \bar{I}(s) ds} \tag{4}$$

where $\bar{I}(s)$ is the smeared intensity, in arbitrary unit. The quantity R is a useful parameter for the characterization of various structures. In an ideal two-phase structure the electron density gradient at the phase boundary is infinity, as a result of which R goes to infinity. If R becomes finite, the electron density changes from one phase to the other continuously

over a transition layer of width E. In other words if R is finite, corrugation at the phase boundary exists. Less the value of R more is the corrugation. Eq. (4), when expressed in terms of x, Misra *et al* [2,3] reduces to

$$R = \frac{3}{2}(2\pi/\lambda a)^2 \frac{\int_0^\infty x^3 \tilde{I}(x)dx}{\int_0^\infty x \tilde{I}(x)dx}. \tag{5}$$

The quantity 'x' used above represents the position coordinate of the scattered intensity from the centre of the primary beam. It is related to the magnitude of the reciprocal vector s and the scattering angle 2θ by the relation

$$s = \frac{2\theta}{\lambda} = \frac{x}{\lambda a} \text{ as } 2\theta \equiv x/a,$$

where a is the distance between the sample and the plane of registration of the scattered ray (i.e. sample counter distance) and x is the vertical height of recording the scattered X-rays from the centre of the X-ray beam.

The integral $\int_0^\infty x \tilde{I}(x)dx$ is called smeared invariant $\tilde{Q}$. For a two-phase system, Debye and Bueche [12] and Porod [1] have developed theories to prove that the smeared invariant for a scattering curve is independent of the shape and size of the particles responsible for scattering. On the other hand, it depends upon the scattering strength of the system which in turn depends on the square of electron density deviation from the mean value. The integral $\int_0^\infty x \tilde{I}(x)dx$ is the integrated smeared scattered energy.

The method for deriving the three-dimensional correlation function $C(r)$ from the smear intensities, was developed by Mering and Tchoubar [13] and expressed in terms of x by Misra *et al* [2,3] as

$$C(r) = \frac{\int_0^\infty x \tilde{I}(x) J_0(2\pi rx/\lambda a)dx}{\int_0^\infty x \tilde{I}(x)dx}. \tag{6}$$

The significance of correlation functions (three- and one-dimensional) can be visualised as follows : Take variable measuring rod and move it in all possible directions for three dimensional correlation function and in one direction perpendicular to the layers. The product of deviation of electron density from the mean value will be positive and negative

for different locations depending whether both the ends fall in same or opposite phases respectively [14,15].

In case of single particle (i.e. for dilute system), $C(r)$ decreases from one to zero as $r \to \infty$ and for other densely packed systems as in our case it oscillates ultimately going to zero. So in such points of 3-dimensional and 1-dimensional correlation functions the first and next consecutive peaks corresponds to consecutive crystalline region.

For a non-ideal two phase structure having continuously varying electron density of width E, the value of E can be calculated from $C(r)$ of the sample normalised to unity at the origin in real space. The equation for calculating E, known as the width of the transition layer, was developed by Vonk [11] and is given by the equation

$$E = -\frac{4}{R}\left(\frac{dC(r)}{dr}\right)_{r} = E_{v}. \tag{7}$$

To calculate E, it is necessary to compute the values of $C(r)$ for various values of r real space.

For a layer structure, Vonk and Kortleve [15] have made use of one-dimensional correlation function $C_1(Y)$. The expression for $C_1(Y)$ as given by Mering and Tchoubar [13] and expressed in the terms of x, leads to

$$C_1(Y) = \frac{\int_0^{\infty} x\ \tilde{I}(x)\,[J_0(z) - zJ_1(z)]dx}{\int_0^{\infty} x\ \tilde{I}(x)dx} \tag{8}$$

where $z = 2\pi xy/\lambda a$. As predicted by Vonk [11], the position of the first subsidiary maxima in the one-dimensional correlation function $C_1(Y)$, give the value of the probable distance between dense particles D, transverse to the layers. The parameter D is the repeat distance between matter to matter or void to void transverse to layers as per the significance of $C_1(Y)$ already mentioned. So the relation

$$\left(\frac{dC_1(Y)}{dy}\right)_{y>E} = -\frac{1}{D}\,\frac{\Delta\eta^2}{\langle\eta^2\rangle} \tag{9}$$

derived by Vonk (11), the value of $\frac{(\Delta\eta)}{\langle\eta^2\rangle}$ can be computed, where $\Delta\eta$ is the electron density difference between two neighbouring phases. For a layer structure, the specific inner surface defined as the phase boundary per unit volume of the dispersed phase is given by Vonk [11] as

$$\frac{S}{V} \quad \frac{2}{D} \tag{10}$$

For a non-ideal two-phase system the relation

$$\langle \eta^2 \rangle = (\phi_1 \phi_2 - \frac{ES}{6v}) \tag{11}$$

is valid as shown by Vonk [11]. In the above relation ϕ_1 and ϕ_2 are the volume fractions of the two phases matter and void respectively. For this calculation, the phase boundary is chosen at the middle of the transition layer. As the sum of volume fractions of the two phases is unity, the values of ϕ_1 and ϕ_2 can be determined by using eq. (11).

Following Porod [1], the distance statistics can also be used for calculation of transversal lengths which are as follows. In an irregular two phase system, if arrows are drawn in all possible directions, the number average of chord lengths through the two phases in all directions are known as transversal lengths denoted by $\bar{l}_1$ and $\bar{l}_2$ [16].

$$\text{Values of } \bar{l}_1 = 4\phi_1 \frac{V}{S}$$

$$\text{and} \qquad \bar{l}_2 = 4\phi_2 \frac{V}{S} \tag{12}$$

derived by Mittelbach and Porod [17]. The above quantities give a measure of the size of the phases as shown by Mittelbach and Porod [17] and the range of inhomogeneity $\bar{l}_r$ is

$$1/\bar{l}_r = 1/\bar{l}_1 + 1/\bar{l}_2 \,. \tag{13}$$

Hence, the range of inhomogeneity $\bar{l}_r$ is analogous to the concept of reduced mass in mechancs and represents an average chord length paramer [77].

It contrast to $\bar{l}_1$ and $\bar{l}_2$, the number average of the thickness of region of the two phases in one dimension transverse to the layers are denoted as $\bar{d}_1$ and $\bar{d}_2$. The one-dimensional average length parameter in this direction is $\bar{d}_r$. The three parameters are related as

$$\frac{1}{\bar{d}_r} = \frac{1}{\bar{d}_1} + \frac{1}{\bar{d}_2} \,. \tag{14}$$

Also the relation

$$\bar{d}_1 = \frac{\bar{l}_1}{2} \text{ and } \bar{d}_2 = \frac{\bar{l}_2}{2} \tag{15}$$

hold good [16].

As shown by Mittelbach and Porod [17] the distance of heterogeneity i.e. length of coherence l_c can be obtained from the following integral

$$l_c = 2\int C(r)\, dr \,. \tag{16}$$

The length of coherence l_c is defined as the mean width of the correlation function and also it is weight average of $\bar{l}_r$ [18]. The quantity f_c, defined as the characteristic number by Porod [1] can be obtained from the equation

$$l_c = \frac{l_c}{2\bar{l}_r} \,. \tag{17}$$

An increase in the above ratio indicates an increase in anisometry (or isometry) in the scattering system and decrease in f_c suggests the decrease in anisometry [19].

A completely different approach for the estimation of the value of the transition layer E, here denoted as E_R, was suggested by Ruland [4]. The functional relation $\tilde{I}(s \to \infty)$ with 's' at the tail end of the SAXS pattern for a non-ideal two-phase system is given by

$$\tilde{I}(s \to \infty) = \frac{\pi c}{2}\left(\frac{1}{s^3} - \frac{2\pi^2 E^2}{3s}\right) \tag{18}$$

where c is the constant of proportionality and E_R goes to zero for an ideal two-phase system. In terms of x variable, the above relation can be written as

$$\tilde{I}(x \to \infty).\, x = \pi c/2\,(\lambda a)^3 x^{-2} - \pi^3 c/3\,(\lambda a)\,E^2. \tag{19}$$

The value of E_R can be calculated from the graph of $\tilde{I}(x \to \infty)\, .x$ versus x^{-2} known as Ruland plot.

5. Background correction

During small angle X-ray scattering data collection, it is frequently found that a continuous background scattering overlaps the SAXS pattern of the sample. The presence of the background scattering introduces error in the calculation of the correlation functions and the width of the transition layer. As suggested by Vonk [11], the correlation function at the origin is sensitive to the error in the tail region of the SAXS curve. Therefore, special care has been taken to separate the SAXS intensities $\tilde{I}(s)$ from the continuous background scattering $\tilde{I}_{bg}(s)$. As reported by Kortleve *et al* [20], the continuons background scattering in the SAXS pattern of some samples show an upward trend at large values of 's' after first passing through a minimum value in the observed SAXS curve. In such a case, the experimentally observed data at the tail end can be fitted to an equation

$$\tilde{I}(s) = a + bs^n \tag{20}$$

where a and b are constants and n is an even positive integer. Further, it was shown by Konrad and Zachmann [21] that $\tilde{I}_{bg}(s)$ remains constant in the region where $\tilde{I}(s)$ contributes appreciably. In such a case a constant background intensity corresponding to the minimum intensity value in the SAXS pattern of the samples Misra *et al* [2,3] can be deducted. Both of the methods used for background correction gave values of E obtained from Vonk and Ruland methods show relatively very small difference. In our calculation, the second method of subtracting the minimum intensity as the background correction has been used with the corrected SAXS intensities being used in subsequent calculations.

6. Calculation and results

The initial four intensity data in the $\tilde{I}(x)$ versus x curve for the case with the fibres parallel to the slits for both samples were fitted to the Gaussian curve [22].

$$\tilde{I}(x \to 0) = P e^{-qx^2}$$

by the least square technique. The values of P obtained were 2859.84 $jm^{-2}s^{-1}$ and 3650.12 $jm^{-2}s^{-1}$ and the values of q obtained were 211.01 m^{-2} and 240.05 m^{-2} respectively for T_a and T_{60}. Taking the values of P and q the scattered intensity curves were extrapolated to zero angle for both samples. The extrapolated points for T_a and T_{60} are indicated by symbols Δ and $\diamond$ respectively, in Figure 1. It may be noted that the methods of extrapolation has very little effect on the relevant part of the correlation function. Neither the position nor the height of the first subsidiary maximum of the one-dimensional correlation function is much affected [3]. The two integrals in relation 5 for the R parameter for both samples were calculated by numerical integraion applying Simpson's one-third rule; the values are 1.46×10^{-3}Å^{-2} and 1.88×10^{-3}Å^{-2} respectively. The small positive values of R for both samples show that the electron density gradient at the phase boundary is finite, establishing that both samples belong to the non-ideal two-phase system. Using eq. (6) the three-dimension correlation function $C(r)$ for both samples were computed for various values of 'r' and is plotted in Figure 2. The slopes of $C(r)$ at different points for both samples were computed by the numerical differentiation method using five point central difference formula with a constant interval of 1 Å. The values of $-(4/R)(dc(r)/dr)$ versus r for both samples are plotted in Figure 3. In the same graph, a straight line equidistant from both axes has been drawn and the point of intersection of this line with the two curves give the values of E referred to as E_v using relation (7). The values obtained for T_a and T_{60} are given in the Table.

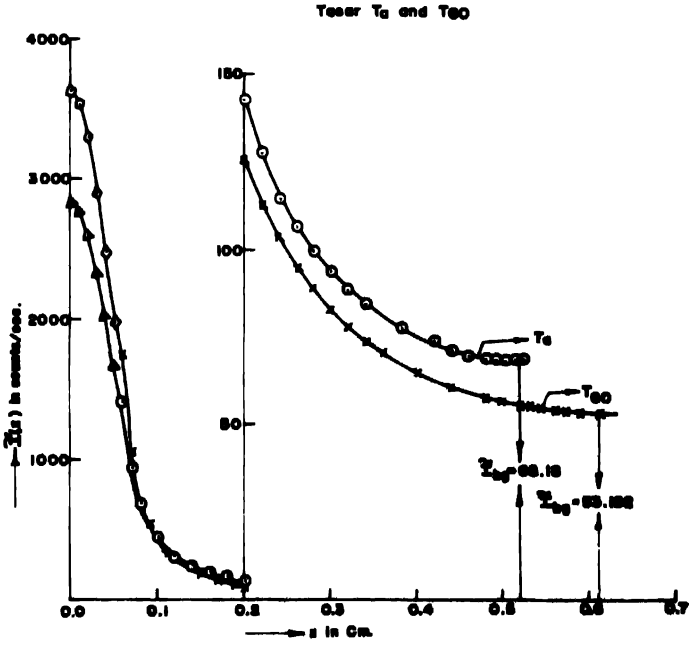

Figure 1. Smeared-out scattering curve magnified from 0.20 cm.

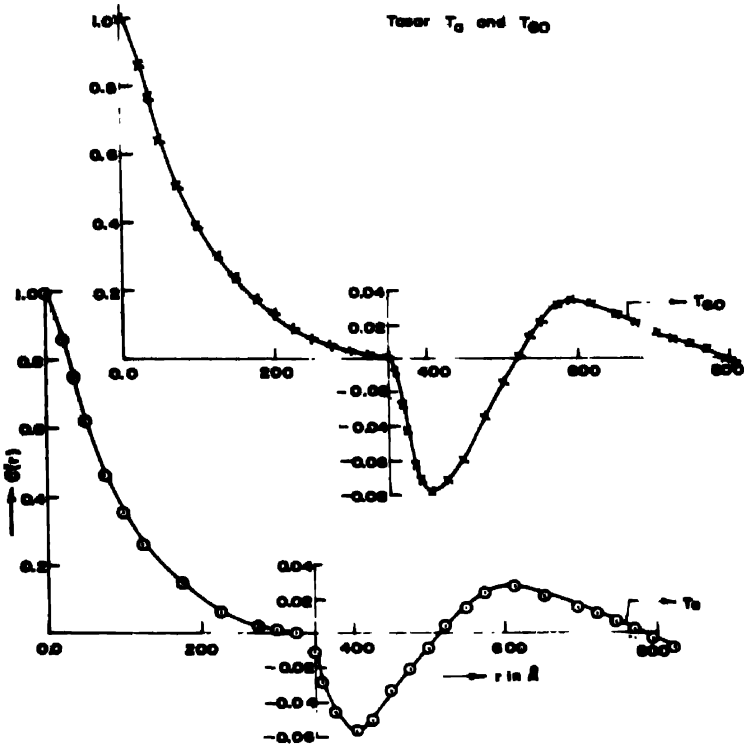

Figure 2. The curves showing the 3-dimensional correlation function $C(r)$ against 'r' values. Both the curves, magnified from 350 Å.

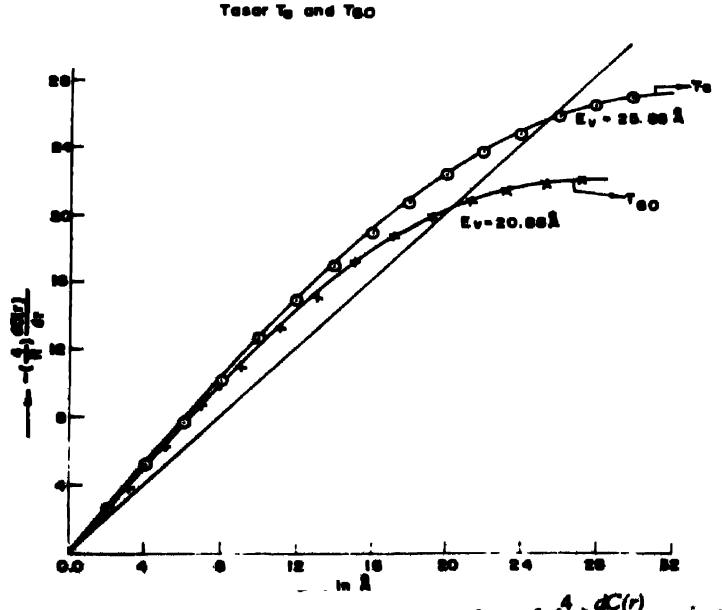

Figure 3. The curves showing the various values of $-\left(\frac{4}{R}\right)\frac{dC(r)}{dr}$ against 'r' values.

Scanning Electron Microscopy (SEM) and Transmission Electron Microscopy (TEM) photographs of tasar sample have been reported by Bhat and Nadigar [23]. They clearly indicate that tasar fibre has a layer structure. To prove the isotropic nature of the samples, scattering patterns of the sample were taken keeping the sample parallel and perpendicular to the primary beam. Both scattering patterns are shown in Figure 7; they are nearly symmetrical in nature, suggesting that the sample is isotropic. Therefore the one-dimensional correlation function applicable to layer structures [15] was calculated for both samples [13]. C_1 (y) versus y is plotted in Figure 4. The values of D, the probable distance between dense particles transverse to the layer for both the samples were obtained from the position of the first subsidiary maximum in the plots of one-dimensional correlation function (Figure 4) are shown in Table 1. From relation (10), the values of S/V, the specific inner surface were obtained for T_a and T_{60} and are displayed in the same table. The values of slopes $\frac{dC_1(y)}{dy}$ were calculated at various points for T_a and T_{60} and were found out to be constant for values of $y > E_v$. Using relation (9) the values of $\frac{\langle \eta^2 \rangle}{(\Delta\eta)^2}$ were

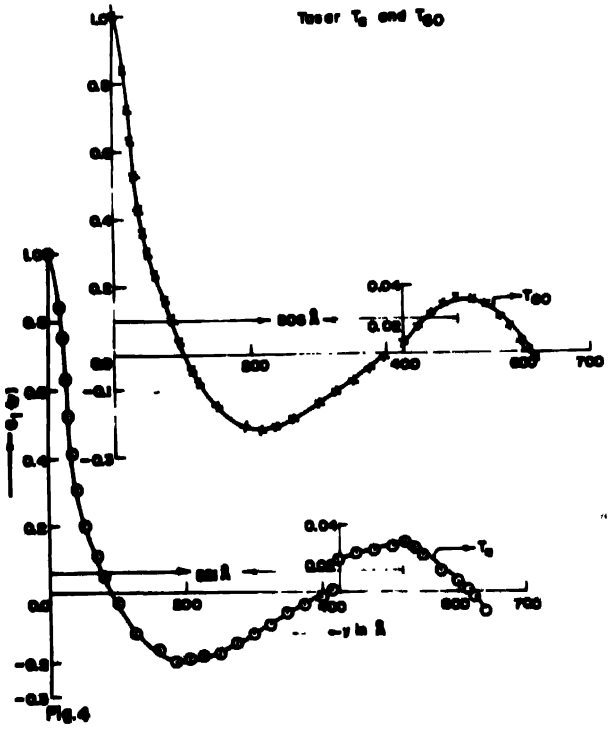

Figure 4. The curves showing the values of one-dimensional correlation function $C_1(y)$ against 'y' values. Both the curves magnified from 425 Å.

obtained for T_a and T_{60} are also included in the table. Assuming $\phi_1 + \phi_2 = 1$ and employing relation (11), the values of ϕ_1 and ϕ_2 for T_a and T_{60} were computed and the values are shown

in the table. From eq. (12) the transversal lengths $\bar{l}_1$ and $\bar{l}_2$ for T_a and T_{60} were found out and are given in the table.

The average values of range of inhomogeneity $\bar{l}_r$ were calculated from eq. (13) for T_a and T_{60} and given in the table. Similarly $\bar{d}_1$, $\bar{d}_2$ and $\bar{d}_r$ have been calculated from relations (14) and (15). The length of coherence l_c was obtained from eq. (16) for T_a and T_{60}, are shown in the table. Using relation (17), the characteristic number f_c were obtained for both the samples and displayed in the table. The values of $2E/D$, the volume fraction of transition layer were computed for both samples and are included in the table. Smeared out invariant and scattered energy due to both the samples as defined in the text were also computed as 9.81, 11.36 and 184.69, 222.55 respectively.

The Ruland plots of $\bar{I}$ ($x \to \infty$) versus x^{-2} are drawn in Figure 5 for both samples. Both plot give straight lines at the tail end of the scattering curve of both samples. The slope and y-intercept, were obtained from the Ruland plot as 1.0 and –3.8 for T_a and 1.11 and –3.4 for T_{60}. Using the values of slopes and y-intercept, the width of transition layer E_R by Ruland method were found out for T_a and T_{60} and are displayed in the table. The standard deviation of the intensities $\sigma\left(\sqrt{\bar{I}}\right)$ at the tail end of the SAXS curve for both samples were calculated and the values obtained are 2.73×10^{-3} and 2.09×10^{-2} and are well within the

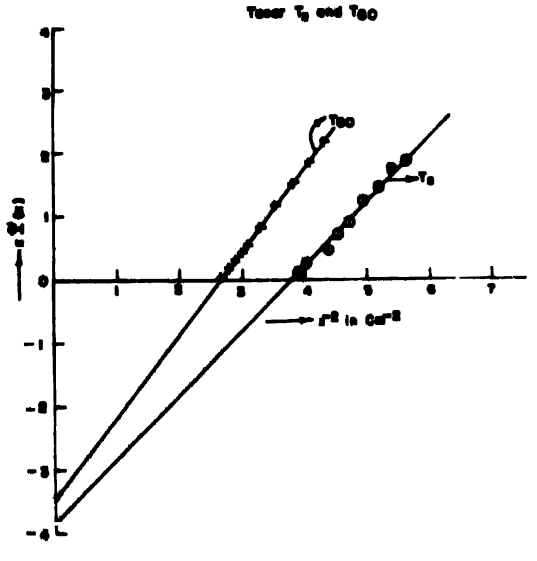

Figure 5. The plot of $x\bar{I}(x)$ vs x^{-2} values.

permissible limit of 0.5. The line of regression of the intensities at the tail end of the SAXS curve for both samples were calculated and the values obtained are 0.9 for both T_a and T_{60} which are very close to the desired value of 1.0 indicating that the intensity data

collected for both the samples [22] are within permissible error.

7. Conclusion

A close scrutiny of all the calculation made above shows that tasar silk should be considered as non-ideal two-phase system. The above conclusion is obtained from the fact that the Ruland plot for an ideal system leads to a straight line without any y-intercept. But the Ruland plots of T_a and T_{60} in Figure 5 give a negative intercept of –3.8 and –3.4 respectively confirming the fact that both samples are non-ideal two-phase systems. The magnitude of the intercept provides a measure of deviation from the ideal to non-ideal system and therefore provides a measure of deviation from the Porod's law. It can be ruled out that for some samples the intercept may be positive leading to two important possibilities, (i) the system may not come under two-phase system, (ii) the dimensions of the scattering particles may be small enough for using SAXS.

As mentioned earlier in the theory the non-ideal two-phase structure is one in which the surface between the matter and void regions are not smooth, but are corrugated. Therefore, between the matter and void phase there occur a region of continuously varying electron density and the width of this region is called transition layer. The width of transition layer is calculated for T_a following Vonk method as E_v = 25.88 Å and Ruland method as E_R = 23.54 Å and similarly for T_{60}; E_v = 20.88 Å and E_R = 19.6 Å. The small difference between the two values obtained by different approaches for both samples indicate the accuracy and the correctness of the data collected and the method of analysis used. All the important macromolecular parameters calculated for both samples are shown below in tabulated form (Table 1).

Table 1. Various parameters obtained in this work.

Parameters	T_a	T_{60}
D	521 Å	506 Å
R	1.46×10^{-3} Å^{-2}	1.88×10^{-3} Å^{-2}
S/V	3.84×10^{-3} Å^{-1}	3.95×10^{-3} Å^{-1}
E_v	25.88 Å	20.88 Å
$\frac{\langle \eta^2 \rangle}{(\Delta\eta)^2}$	0.17	0.16
ϕ_1	0.75	0.78
ϕ_2	0.25	0.22
$\bar{l}_1$	781.22 Å	789.36 Å
$\bar{l}_2$	260.76 Å	222.64 Å
$\bar{l}_r$	195.51 Å	174.26 Å
$\bar{d}_1$	390.61 Å	394.68 Å
$\bar{d}_2$	130.38 Å	111.32 Å
$\bar{d}$	97.75 Å	87.13 Å
$2E/D$	9%	8%
l_c	184 Å	192 Å
f_c	0.47	0.55
E_R	23.54 Å	19.6 Å

The lamellar model based upon above findings is shown in Figure 6 and supported by TEM photograph [23]. The $C(r)$ versus 'r' plot shows damped oscillatory behaviour as

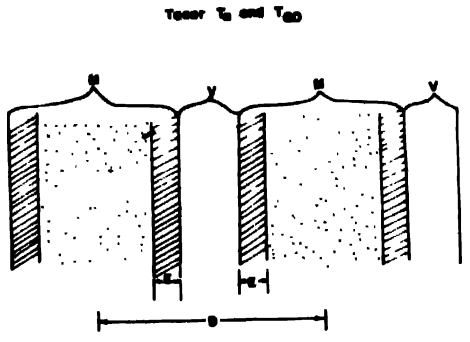

Figure 6. Lamellar model, not to scale.
M, matter; V, void; D, periodicity transverse to the layer; E, width of transition layer.

found by Misra *et al* [2] for non-ideal two-phase systems and the same trend is evident for both samples. In the model (Figure 6), D has been shown as the distance between the mid points of two consecutive matter regions. So the parameter $2E/D$ in percentage, the volume fraction of transition layer, E occurs twice. Work on tasar samples is in progress under

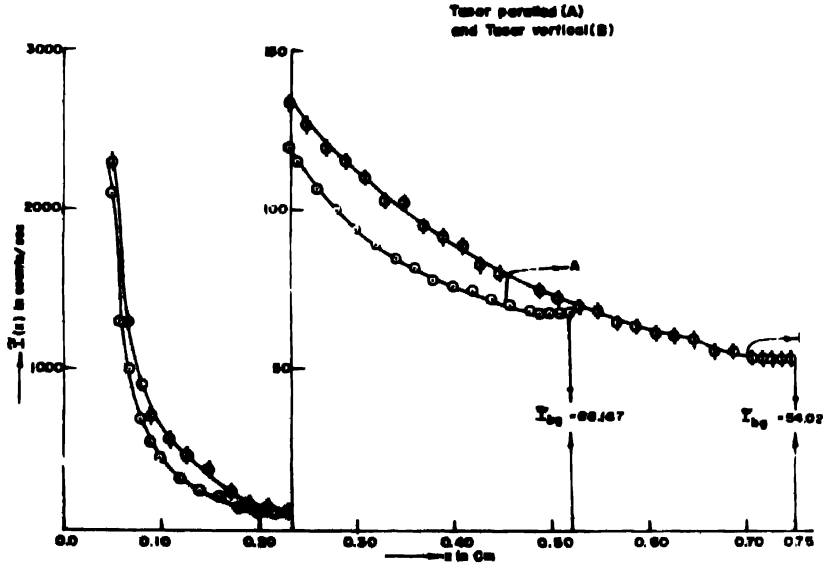

Figure 7. The curves showing the values of $I(x)$ *vs* x keeping the sample to be parallel (A) and vertical (B) to the primary beam. Both the curves magnified from 0.23 cm.

different physical conditions and chemical treatments. In future, we will be in a position to provide much more information and establish some relation between the results obtained and the fibre properties of tasar.

Acknowledgment

We are thankful to the Principal, Prof S Misra, Regional Engineering College, Rourkela for his encouragement and granting permission to A K Sahoo for utilising the facilities of the Physics Department.

References

[1] G Porod 1951 *Kolloio-z* 124 83; 1952 *Liquid* 125 51
[2] T Misra, K C Patra and T Patel 1984 *Colloid Polym. Sci.* 262 611
[3] T Misra, D K Bisoyi, T Patel, K C Patra and A Patel 1988 *Polym. J.* 20 739
[4] W Ruland 1971 *J. Appl. Cryst.* 4 70
[5] A N J Heyn 1948 *Text. Res. J.* 19 163
[6] A N J Heyn 1948 *J. Am. Chem. Soc.* 71 1873
[7] J M Mathews 1954 *Textile Fibres* (New York : John Wiley) 6th ed. p 19, 784, 1099
[8] T Ratho, A Patel and O P Singal 1974 *J. Polym. Sci. Polym. Chem. Ed.* 12 2595
[9] L V Azaaroff and M Z Buerger 1958 *The Powder Method in X-ray Crystallography* (New York : McGraw Hill) p 34
[10] T F Kumosinski, H Pessen, H M Farrell (Jr) and H Brumberger 1988 *Archives of Bio-chemistry and Biophysics* 266 2 548
[11] C G Vonk 1973 *J. Appl. Cryst.* 6 81
[12] P Debye and A M Bueche 1949 *J. Appl. Phys.* 20 518
[13] J Mering and D Tchoubar 1965 *J. Appl. Cryst.* 1 153
[14] A Guinier and G Fournet 1955 *Small angle X-rays* (New York : John Wiley) p 78
[15] C G Vonk and G Kortleve 1968 *Kolloid Z. Z. Polym.* 225 124
[16] W Ruland 1977 *Colloid Polymer Sci.* 255 417
[17] P Mittelbach and P Porod 1965 *Kolloid Z. Z. Polym.* 202 40
[18] O Glatter and O Kratky 1982 *Small angle X-ray Scattering* (New York : Academic) p 29
[19] T Ratho and B C Panda 1965 *Indian J. Phys.* 39 207
[20] G Kortleve, C A F Tuynman and C G Vonk 1972 *J. Polym. Sci.* 4210 851
[21] G Konrad and H G Zachmann 1971 *Kolloid Zuz Polym.* 247 851
[22] C G Vonk 1975 *J. Appl. Cryst.* 8 340
[23] N V Bhat and G S Nadigar 1978 *Textile Res. J.* 48 685